

Towards Improved Euro-Mediterranean Discharge Simulations in Regional Coupled Climate Models: A Comparative Assessment of Hydrologic Performance

Mohamed Hamitouche^{1,2,3}, Giorgia Fosser¹, Arezoo RafieeiNasab⁴, Alessandro Anav^{2,3}

5 ¹University School for Advanced Studies IUSS, Pavia, Italy

²Climate Modeling Laboratory, ENEA – Italian National Agency for New Technologies, Energy and Sustainable Economic Development, CR Casaccia, Viale Anguillarese 301, 00123 Santa Maria di Galeria, Rome, Italy

³ICSC Italian Research Center on High-Performance Computing, Big Data and Quantum Computing, Bologna, Italy

⁴Research Applications Laboratory, NSF National Center for Atmospheric Research, Boulder, Colorado, USA

10 *Correspondence to:* Mohamed Hamitouche (mohamed.hamitouche@iusspavia.it)

Abstract. River discharge into the Mediterranean Sea is a vital component of the regional water cycle, influencing ecological and climatic dynamics. Although some regional coupled models that include a river routing component exist for the Mediterranean region, their performance in reproducing river discharge is poor. This study compares the hydrological routing models CaMa-Flood and WRF-Hydro for discharge simulations into the Mediterranean Sea, with the prospect of future coupling into regional and Earth system models such as ENEA-REG. Evaluating their performance across key basins, this study highlights CaMa-Flood's computational efficiency but underperformance in flow variability and high-flow extremes, contrasted by WRF-Hydro's superior timing and bias reduction, especially after calibration. In fact, results indicate that the calibration improved WRF-Hydro's metrics, including Kling-Gupta Efficiency (KGE) and lag times, underscoring its potential for precise discharge predictions at higher computational costs. These findings offer critical insights for advancing regional coupled Earth system models, enhancing hydrological forecasting, and addressing basin-specific hydrological challenges.

1 Introduction

River discharge into the Mediterranean Sea is a critical component of its water budget, alongside the net inflow from both the Atlantic through the Strait of Gibraltar and the Black Sea via the Dardanelles Strait, as well as evaporation and precipitation (Pinaridi et al., 2015; Pinaridi and Masetti, 2000). As one of the primary freshwater sources, river discharge plays a pivotal role in shaping the basin's hydrological and ecological dynamics. Not only it does provide essential freshwater input, particularly during spring when plentiful precipitation rates and snowmelt enhance the discharge, but also transports nutrients and minerals that influence coastal and sub-basin ecosystems (Struglia et al., 2004). Moreover, variability in river discharge, whether natural or anthropogenic, can modulate the Mediterranean's thermohaline circulation on decadal scales, affecting salinity, dense water formation, and oxygenation rates across the basin (Zavatarelli et al., 1998).

Timely and accurate river discharge estimates into the Mediterranean are critical for managing water resources and related risks in the region (Cisterna-García et al., 2025). In a broader context, understanding the interplay between regional climate change and hydrological processes is essential, and underscores the need to study the coupling of Earth system components, including atmospheric, hydrological, and oceanic processes. Since the early 21st century, major international research programs such as WCRP (World Climate Research Programme), IGBP (International Geosphere-Biosphere Program), GEWEX (The Global Energy and Water Cycle Experiment) and CORDEX (COordinated Regional climate Downscaling EXperiment) have emphasized the importance of integrating regional climate models (RCMs) with hydrology and ocean models to address these challenges. Coupled atmospheric-hydrological-ocean models provide a framework to simulate the full water cycle and its feedback mechanisms between land, atmosphere and ocean. Such models reveal how terrestrial water flows influence the broader water cycle and regional climate dynamics over seasonal to decadal scales. For example, terrestrial water flow can alter atmospheric boundary layers and modulate convective precipitation during shorter time scales (Amelia, 2022). By enhancing the representation of water cycle processes, these coupled models aim to improve simulation accuracy and forecasting capabilities. This evolution from traditional hydrological models to coupled models reflects the growing need for tools that capture the intricate interactions between land, ocean, and atmosphere, offering enhanced weather forecasts and improved predictions of river flow and extreme events.

Regional coupled models and climate change studies in the Mediterranean require a high-resolution discharge component to correctly reproduce the complex orography and land-sea distribution of the Mediterranean region and thus effectively close the coupling among the Earth system components (Hagemann et al., 2020). However, the first coupled models did not consider the hydrological component and the coupling was limited to atmosphere-ocean-land only (e.g. RegIPSL (Shahi et al., 2022), EBU-POM (Djurdjevic and Rajkovic, 2010) and MORCE (Drobinski et al., 2012)), where rivers are inadequately represented. This restricts their ability to make accurate predictions of river flow and forecasts for floods and droughts, necessitating downstream hydrological modelling, independently of land-atmosphere feedback or the advantages of data assimilation. Additionally, while some models incorporate atmosphere-ocean-land-river coupling, they struggle to meet the high-resolution requirements essential for precise discharge simulations.

Recent advances have led to the development of several complex coupled models, aimed at achieving fully integrated hydrological predictions for the Mediterranean region. Despite the sophistication to simulate complex earth system interactions, these models still face significant challenges. In particular, some models systematically underestimate freshwater input from river runoff, leading to inaccuracies in discharge predictions and contributing to surface water salinification in the Mediterranean (Anav et al., 2021; Reale et al., 2020; Storto et al., 2023). This underestimation seems to be with the Hydrological Discharge (HD) model (Hagemann and Dümenil, 1997), a river routing model used to simulate the river discharge with different horizontal resolutions (e.g. 5 minutes in MESMAR and 0.5 degrees in ENEA-REG coupled models). The HD model uses a pre-parametrization based on a linear reservoir routing concept with pre-defined reservoir numbers and temporal constants tailored to runoff inputs from the HydroPy Land Surface Model (LSM) (Stacke and

Hagemann, 2021), which neglects the energy budget and overestimates runoff. Consequently, replacing the biased routing
65 model in these coupled systems has become essential to ensure a more accurate representation of the water cycle.
At the same time, enhancing discharge simulations would also benefit from selecting the most appropriate land surface
runoff model based on its runoff generation mechanism. A recent study by Hamitouche et al. (2025a) analysed the impact of
seven different runoff schemes within the Noah-MP LSM on global discharge simulations across diverse climate regions and
found that the Schaake runoff scheme performed best in warm temperate regions, including the Mediterranean basins. This
70 study utilized the CaMa-Flood hydrodynamic model (Yamazaki et al., 2011) for discharge simulation, demonstrating overall
good performance against observational discharges. However, the analysis also revealed certain limitations, such as delays in
capturing seasonal peak flows due to inherent constraints in CaMa-Flood, which were accurately resolved by the WRF-
Hydro model (Gochis et al., 2021), tested in the same study. Additionally, the study identified significant biases, particularly
in high-flow extremes, emphasizing the need for ongoing calibration of tuneable parameters to improve the accuracy of
75 hydrological predictions.
This highlights the importance of thoroughly evaluating standalone routing models for their performance and limitations,
before integrating them into regional coupled climate or Earth system models—such as the ENEA-REG atmosphere-land-
river-ocean (ALRO) coupled model, developed within the framework of the Mediterranean CORDEX (Med-CORDEX)
initiative. Med-CORDEX aims to advance fully coupled regional climate simulations over the Euro-Mediterranean domain,
80 which encompasses the Mediterranean and Black Seas and their contributing catchments (excluding the Nile), by improving
the representation of key Earth system components, including atmospheric processes, land surface, hydrology and ocean
dynamics (Ruti et al., 2016). The Med-CORDEX Phase 3 protocol outlines common requirements for domain extent, spatial
resolution, and coupling strategies—mandating, for example, a minimum resolution of 12 km for the atmosphere/land and 10
km for the ocean, and requiring river-to-ocean coupling. Further details on the protocol are available at
85 <https://zenodo.org/records/11659642>.
Considering the poor performance in reproducing accurate discharge estimates as well as some limitations of the existing
regional coupled model for the Mediterranean region, the aim of this study is to compare the performances of two process-
based hydrological routing models, i.e. CaMa-Flood and WRF-Hydro, driven by a Med-CORDEX regional coupled model
(ENEA-REG), in reproducing the discharge for the most important Mediterranean rivers. This evaluation provides valuable
90 information, as the analysed models could be regarded as alternatives to the river component used in current regional
coupled models. CaMa-Flood, a global river routing model, is widely recognized for its computational efficiency and ability
to simulate river discharge at large scales. However, within the Med-CORDEX domain (Fig. 1), it has been utilized only
outside the context of regional coupled models. On the other hand, WRF-Hydro, the hydrological extension of the WRF
atmospheric model, is designed for high-resolution hydrological predictions, with multi-scale capabilities, enabling it to
95 represent processes on various spatial scales (Gochis et al., 2021). Over the Mediterranean region, its application has
primarily been limited to small isolated and relatively undisturbed basins, and short time periods (Galanaki et al., 2021;
Senatore et al., 2015; Sofokleous et al., 2023, 2024). In contrast, in this study, simulations were conducted at a daily time

scale over a long-term period (1990-2014) for the entire Med-CORDEX domain. The evaluation focused on several Mediterranean basins as well as the Danube River, which drains into the Black Sea, allowing for robust regional generalizations and comparative analyses across diverse hydrological regimes. Additionally, the study analyzed the role of parameter calibration in improving discharge simulations, with a particular focus on WRF-Hydro, leveraging the capabilities of the NCAR WRF-Hydro calibration package.

This study addresses the following key questions:

- Can WRF-Hydro or CaMa-Flood serve as effective alternatives to improve hydrological simulations within Euro-Mediterranean regional coupled models?
- Can calibration enhance WRF-Hydro performance, and to what extent?

The paper is structured as follows: after the presentation of the used models and methods (section 2), the first part of result (section 3.1) focuses on comparing the two hydrological models in their default configurations, offering insights into the foundational performance of these models. This approach establishes a basis for comparison and lays the groundwork for future studies to refine and adapt these models for innovative applications, particularly in Mediterranean hydrological and climatic contexts. The second part of the results (section 3.2) evaluates the impact of calibration in further improving discharge simulations, highlighting the potential of parameter optimization to enhance hydrological model performance, focusing on WRF-Hydro, by leveraging the capabilities of the NCAR WRF-Hydro calibration package.

2 Materials and methods

2.1 Study area and river discharge observations

The river basins draining into the Mediterranean Sea encompass over 5 million km², including the Nile basin, but excluding rivers flowing into the Atlantic Ocean from Portugal and Spain (Lionello et al., 2012; Ludwig et al., 2009). Most of these catchments are medium to small-scale, with only a few major basins exceeding 80,000 km² (Lionello et al., 2012). The ten largest rivers contributing to Mediterranean discharge include Rhone, Po, Drin-Buna, Nile, Neretva, Ebro, Tiber, Adige, Seyhan and Ceyhan rivers (Ludwig et al., 2009), with 71% of the total discharge originating from northern Mediterranean countries, 12% from eastern regions (Turkey), and 17% from southern areas, primarily the Nile. Notably, the Rhone and the Po alone contribute 25% of the northern discharge. Annual freshwater input to the Mediterranean and Black Sea is estimated at 305–737 km³/year (Struglia et al., 2004).

The ENEA-REG model (Anav et al., 2021), developed within the Med-CORDEX framework, incorporates into its ocean component river discharge from 18 major Mediterranean rivers simulated by the river routing component. Among these are several of the largest Mediterranean rivers—Rhone, Po, Ebro, Adige, Tiber, and Ceyhan—along with additional basins such as Drin, Maritsa, Goeksu, Vjosa, Jucar, Buyuk Menderes, Arno, Koprui, and Struma. For the Nile, a climatological monthly mean is prescribed, as suggested by the Med-CORDEX protocol (<https://zenodo.org/records/11659642>), due to the

atmospheric model's limited domain coverage of the basin and the significant anthropogenic modifications to its natural
130 discharge.

In this study, the validation focuses on 10 of the ENEA-REG routed rivers, in addition to the Danube River (Fig. 1), chosen
based on the availability of at least five consecutive years of daily observations after 1990. These rivers include: Maritsa,
Goeksu, Arno, Kopru, Rhone, Po, Ebro, Ceyhan, Adige, and Tiber. Notably, six of these (Rhone, Po, Ebro, Tiber, Adige, and
135 Ceyhan) are also among the ten largest Mediterranean rivers listed earlier, providing a representative mix of major and
medium-sized basins. The selected rivers span different climatic and morphologic conditions, ranging from mountainous
alpine regions with pluvio-nival hydrological regimes (e.g., Rhone, Po, Adige) to the semi-arid climate of southern Turkey's
Ceyhan River. Other river basins were excluded due to insufficient daily observational data or records shorter than five
years.

The Júcar and Nile rivers were specifically excluded because their flow is heavily influenced by human interventions, such
140 as reservoirs and water diversions, which are not explicitly represented in the modelling setup. In the case of the Júcar, its
relatively small drainage area (22,200 km²) combined with an exceptionally dense and complex regulation system—
including major reservoirs for flood control and water supply (e.g., Alarcón, Contreras, Tous, Bellús, Forata), hydropower
reservoirs (e.g., Molinar, Cortes, Naranjero, La Muela), additional smaller reservoirs, river–aquifer connections, and inter-
basin water transfers (Momb Blanch et al., 2014; Suárez-Almiñana et al., 2017)—strongly alters both the magnitude and timing
145 of discharge. These extensive modifications suppress the natural hydrological signal, making it difficult for hydrological
models to reproduce even the basic flow variability when compared with observations; meaningful validation is therefore not
feasible under the present modelling configuration. For the Nile, in addition to the substantial anthropogenic modifications
along its course, the Med-CORDEX atmospheric domain does not cover the full basin, which is why the protocol prescribes
a monthly climatological discharge. As a result, the Nile cannot be included in the validation of dynamically simulated river
150 flows.

For each selected river, simulated discharge was compared to observations from the nearest available station to the river
mouth, covering upstream areas between 1,900 and 95,000 km² (807,000 km² for the Danube). Observational data were
sourced from the Global Runoff Data Centre (GRDC, 2024), the Hydrographic Studies Center of CEDEX (CEH-CEDEX,
2024), and from Hagemann et al. (2020). To ensure accurate hydrograph construction and validation metrics, simulated
155 discharge values corresponding to missing observational data were removed.

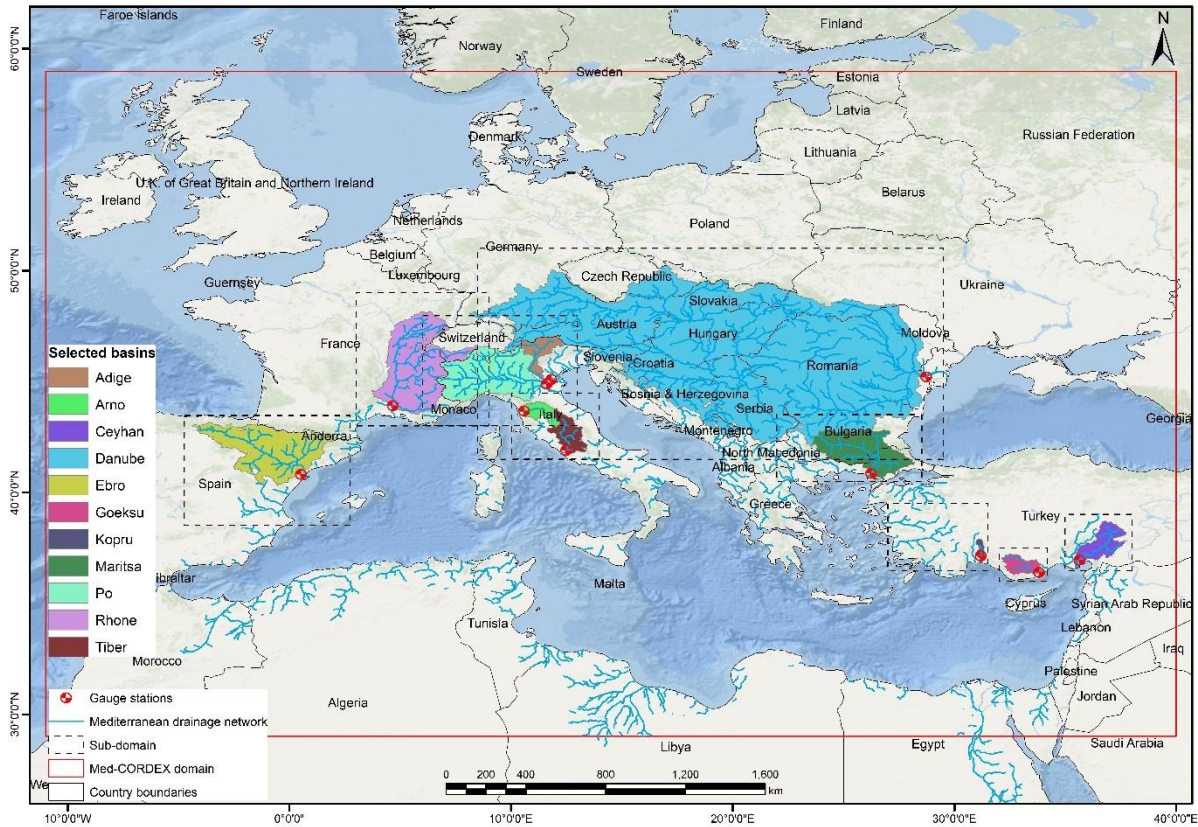


Figure 1: Med-CORDEX simulation domain with its drainage network and the gauge stations (red dots) used in this study. The selected basins for evaluation and calibration are given distinct colours. The dashed contours refer to calibration sub-domains.

2.2 Model description and experimental setup

160 This study is based on the use of CaMa-Flood and WRF-Hydro hydrological models for daily discharge simulations, driven by the ENEA-REG atmosphere-land-ocean coupled model run at 12km resolution over the Med-CORDEX domain. Within ENEA-REG, WRF model is used to dynamically downscale ERA5 data (Hersbach et al., 2020) and simulate the atmospheric variables, while the Noah-MP model simulates the runoff. The configurations of both models (WRF and Noah-MP) are provided in Table S1 and Table S2 in the supplement. All the ENEA-REG variables required as input by the two hydrological models are previously regridded to 6 km resolution using conservative remapping. In particular, CaMa-Flood uses as input daily runoff (surface + subsurface runoff, Fig. S1 in the supplement), while WRF-Hydro, which couples Noah-MP with the hydrological routing model, requires a set of atmospheric state variables —such as air temperature, surface pressure, specific humidity, horizontal wind components (10 m), downward shortwave and longwave radiation, and rainfall rate— provided at 6-hourly intervals (Fig. S2 in the supplement).

170 To guide the reader through the experimental design, we structured the modelling experiments from the simplest to the most complex configuration. First, we evaluate the ENEA-REG-driven CaMa-Flood and WRF-Hydro in their default setups,

ensuring a fair comparison between the two models. These default configurations, described in Sections 2.2.1 and 2.2.2, constitute the core model intercomparison of this study. In a second step (Section 2.2.3), we introduce an additional level of complexity by calibrating key hydrological parameters of WRF-Hydro. This supplementary analysis assesses how much
175 calibration can further enhance discharge performance, providing insight into potential improvements when computational resources permit.

Both CaMa-Flood and WRF-Hydro hydrological models are run for the period 1990-2014, after five years of spin-up. None of the simulations considers reservoir operations and lakes, due to the lack of consistent and comprehensive information on reservoir management and characteristics across all Mediterranean basins. This choice ensures a fair spatial evaluation across
180 the study domain, but we acknowledge it as a limitation that may contribute to reduced performance in some rivers.

2.2.1 CaMa-Flood processes and configuration

CaMa-Flood (v4.11, Yamazaki et al., 2011, 2013) is a global-scale distributed hydrodynamics model designed to simulate river discharge, water levels, and floodplain inundation by routing runoff from land surface models through a predefined river network map. The model employs a Manning's friction coefficient of 0.03 for main river channels and automatically
185 adjusts its routing time step to satisfy the Courant-Friedrichs-Lewy condition as used in previous studies (e.g., Bates et al., 2010; Yamazaki et al., 2013).

CaMa-Flood employs the local inertial equation (a simplified form of the Saint-Venant equation that excludes the advection term) to balance computational efficiency with physical accuracy. River basins are represented as unit catchments with subgrid parameters for floodplain topography, allowing floodplain inundation to be modelled as a subgrid-scale process.
190 River discharge is calculated between upstream and downstream catchments based on the grid-vector hybrid river network, while water levels and inundation areas are diagnosed from water storage in each catchment, assuming uniform water surface elevation. Water storage is updated by conserving mass, incorporating upstream inflows, downstream outflows, and local runoff inputs. Floodplains of neighbouring unit catchments can exchange flows through so-called bifurcation channels, making it a quasi-2D model.

195 The river network map and subgrid topography parameters were extracted using the FLOW upscaling algorithm (Yamazaki et al., 2009), applied to MERIT Hydro hydrography maps (Yamazaki et al., 2019) and MERIT DEM data at 3 arcsec (90 m) resolution. Errors and obstacles in the DEMs, such as vegetation canopy, levees, water surface contamination, and radar speckles, were corrected to ensure consistent downhill flow along streamlines (Yamazaki et al., 2012).

2.2.2 WRF-Hydro processes and configuration

200 WRF-Hydro (v5.2, Gochis et al., 2021) is a hydrological model designed to simulate surface and subsurface runoff processes, either as a standalone model as in our case or coupled with the WRF atmosphere model. It integrates overland flow, subsurface flow, baseflow, and channel routing to represent river discharge and hydrodynamics. WRF-Hydro solves the Boussinesq equation for saturated subsurface lateral flow, accounting for hydraulic gradients driven by topography,

saturated soil depth, and hydraulic conductivity. It incorporates exfiltration from fully saturated cells and infiltration excess
205 from the integrated Noah-MP land surface model (LSM), ensuring a dynamic interaction between surface and subsurface
processes that together contribute to the 2-D overland flow and the 1-D channel routing.

Overland and channel flows are computed using the diffusive wave equation, an efficient approximation of the Saint-Venant
equations that captures backwater effects and shallow water dynamics. The current surface water representation assumes
one-way water flow into channels, without simulating overbank flow. Additionally, baseflow is represented using a
210 conceptual storage-discharge bucket model, which gradually returns water to downstream channels.

Both the land surface model (LSM) and the hydrological routing model components of WRF-Hydro were run on the same 6
km spatial resolution grid. The land surface simulations were conducted at hourly intervals, while discharge was routed
using a conservative terrain and channel routing timestep of 6 minutes. Streamflow outputs were recorded at a daily
frequency.

215 For a fair comparison, WRF-Hydro was run using the same topography generated for CaMa-Flood. However, because WRF-
Hydro requires high-resolution topography to generate the drainage network through its GIS preprocessing tool, the upscaled
DEM was reconditioned both automatically and manually. This reconditioning was based on an available validated drainage
network at a close resolution of $1/16^\circ$ (Wu et al., 2012) and involved minimal intervention to avoid significantly altering
flow velocity.

220 **2.2.3 WRF-Hydro Calibration**

Hydrological models, whether physical or conceptual, require calibration to achieve reliable streamflow simulations. This
necessity arises from two key challenges: (i) the inability to measure all model parameters at the scale of application, and (ii)
the simplification and spatiotemporal discretization of the complex and highly variable rainfall-runoff processes (Beck et al.,
2020).

225 To maintain a fair and balanced comparison between the two models evaluated in this study, the WRF-Hydro calibration is
presented as a distinct and complementary analysis rather than as part of the core intercomparison. This decision reflects
several methodological and practical constraints. Unlike WRF-Hydro, neither CaMa-Flood nor the Noah-MP LSM currently
allows basin-specific or spatially variable parameter calibration, and Noah-MP is not two-way coupled with CaMa-Flood in
our framework. Additionally, calibration of WRF-Hydro was feasible due to the availability of the PyWRFHydroCalib
230 package, whereas no equivalent calibration tool exists for CaMa-Flood. Given the substantial computational cost of regional-
scale calibration, we therefore present the WRF-Hydro calibration results as an “add-on” analysis, illustrating the potential
benefits where resources permit while keeping the main model comparison consistent and unbiased.

The WRF-Hydro modelling system includes various predefined hydrological parameters, some of which are influenced by
land use (e.g., vegetation type and density) and soil type (e.g., silt, clay, loam, sand) (Cerbelaud et al., 2022; Verma and J.,
235 2023). These parameters can be adjusted or calibrated to account for the specific regional orographic and climatic
characteristics (Lahmers et al., 2019; Yu et al., 2023), such as those of the Mediterranean basin, where default parameter

values are often insufficient. Calibration involves determining optimal tuneable coefficients by proportionally adjusting these spatial parameters relative to their default values, ultimately improving simulation accuracy (Cerbelaud et al., 2022; Verma and J., 2023). The WRF-Hydro calibration parameters are categorized into six groups related to: soil properties, runoff
240 processes, groundwater dynamics, vegetation behaviour, snowpack melting, and channel characteristics. In this study, calibration focused on the first four groups, covering 16 parameters (Table S3), while snowmelt parameters were left at their default settings to ensure consistency across basins and fairness in the intercomparison, and for potential future regionalization over other snow-free basins. We acknowledge that this choice may limit performance in snow-influenced basins and that future work could further refine results by including these parameters. Similarly, channel parameters, such as
245 channel roughness, were not calibrated because the channel routing resolution of ~6 km was considered too coarse for a reliable hydrological calibration.

For the calibration of the WRF-Hydro model, the Dynamically Dimensioned Search (DDS) algorithm, a heuristic single-solution-based global optimization method developed by Tolson and Shoemaker (2007), was employed by running the NCAR's (National Centre for Atmospheric Research) PyWrfHydroCalib package
250 (<https://github.com/NCAR/PyWrfHydroCalib>). This algorithm is particularly suited for complex, high-dimensional hydrological models, enabling efficient exploration of parameter space while minimizing computational demands. DDS begins with a global search that transitions to a more localized search as iterations progress, guided by a scalar neighbourhood size perturbation parameter, which is typically set to 0.2. The dynamic adjustment of search size and probabilistic selection of parameters ensure rapid convergence toward good local or regional global optima, even without
255 explicitly targeting the true global optimum (Tolson and Shoemaker, 2007). The stopping criterion is the number of user-defined iterations, which was set to 350 in this study. The calibration objective function, the Kling-Gupta Efficiency (KGE) (Gupta et al., 2009), is optimized to maximize agreement between simulated and observed streamflow. This method has been shown to yield efficient solutions for WRF-Hydro (Cosgrove et al., 2024; RafieeiNasab et al., 2025), balancing computational efficiency with calibration accuracy.

260 Additionally, to address the computational challenges posed by the WRF-Hydro model's complexity and the grid-based structure, which results in longer simulation times compared to other hydrological models (Kiliçarslan, 2022), a sub-domain approach was adopted to optimize calibration efficiency. Instead of calibrating the hydrological basins across the entire Med-CORDEX domain, smaller sub-domains (Fig. 1) were created. Each sub-domain focused on one or two basins (when their calibration date ranges overlapped) and was designed to closely match the Med-CORDEX grid, albeit with minor deviations.
265 Calibration was then performed independently for each basin using an HPC system to ensure efficient utilization of computational resources. On average, the calibration simulations required a bit less than 3000 CPU hours per basin, effectively balancing performance and scalability to address the varying sizes and computational demands of the river basins. Following calibration, the optimized parameters for each basin were reintegrated into the larger Med-CORDEX domain for validation.

270 Before calibration, WRF-Hydro, driven by a regional coupled model (ENEA-REG), was “spun-up” for five years using
default model parameters for each selected basin. This spin-up phase was critical for stabilizing soil moisture initial
conditions. The model state at the end of this spin-up period served as a “warm start” for the calibration phase, which was
performed for five years for each basin. Each calibration iteration included a one-year spin-up as an acclimation phase to
275 RafieeiNasab et al., 2025). The specific spin-up and calibration periods varied across basins and were selected based on the
availability of reliable and continuous observational records (i.e. at least 5-year all falling within the 1990–2014 period), and
are provided in Table S4 in the supplement. The optimized parameters from the calibration were then used to evaluate the
model over the entire available period within 1990–2014, focusing on ensuring consistent performance across the selected
basins. Although this evaluation is not fully independent—since the 5-year calibration window is included—it remains
280 largely independent, given the 25-year evaluation window, and was chosen, in line with previous literature (e.g. Cosgrove et
al., 2024), to ensure methodological consistency with the default (non-calibrated) WRF-Hydro evaluation, performed over
the same full period. This alignment enables a direct, like-for-like assessment of the improvements attributable solely to
calibration. Station-observed streamflow data served as the reference for both calibration and validation, providing a robust
basis for model evaluation. Figure S3 in the supplement summarizes the different calibration steps.

285 **2.3 Metrics**

The evaluation of the performance of the different hydrological models relied on several complementary metrics to capture
various aspects of hydrological behaviour, including correlation, bias, and flow variability. The metrics used in this study are
described below:

1. Spearman’s Rho (Spearman, 1904):

290 This non-parametric measure of rank correlation assesses the monotonic relationship between simulated and observed
streamflow, providing insight into the consistency of flow ranking without assuming linearity. Spearman’s rank-order
correlation coefficient, used as an indication of flow timing, was chosen instead of Pearson’s coefficient due to its
effectiveness in handling nonlinear and non-normally distributed data, such as hydrologic time series (Yue et al., 2002).

2. Kling-Gupta Efficiency (KGE) (Gupta et al., 2009):

295 The KGE was used as a comprehensive measure of model performance, combining correlation, bias, and variability.

3. Relative Standard Deviation (rSD):

The rSD compares the variability in simulated and observed streamflow, expressed as a ratio between the standard deviations
of the simulated and observed streamflow.

4. Percent Bias (%Bias): The %Bias quantifies the systematic error in the simulation as a percentage of observed values.

300 This metric, highlights over- or underestimation of the total flow by the model.

5. Low-flow Percent Bias (Bottom 30%) (Casper et al., 2012):

This metric evaluates the model's ability to simulate long-term low-flow conditions by calculating the bias for the bottom 30% of observed streamflow values, which are critical for drought analysis and ecological studies.

6. High-flow Percent Bias (Top 2%) (Yilmaz et al., 2008):

305 To assess the model's performance in simulating peak discharge events, the bias for the top 2% of observed streamflow values was computed. This is particularly important for understanding flood dynamics and extreme events.

7. Time Lag:

The lag corresponding to the highest cross-correlation between observed and simulated streamflow was calculated to assess the timing discrepancies. This metric helps identify whether the model captures the correct temporal alignment of flow dynamics with observations.

310 Together, these metrics provide a comprehensive evaluation framework, addressing different aspects of hydrological performance, from overall state to extreme conditions. Their corresponding value ranges and equations are detailed in Table 1.

315 **Table 1: List of evaluation statistical metrics. In particular, d is the difference in independent ranking for simulated and observed values for day i and n is the number of values in each time series. σ_{sim} and σ_{obs} are the standard deviations of the simulated and observed streamflow, respectively. QO_i and QS_i are observed and simulated flow values for day i , respectively. r is the Pearson correlation coefficient, β is the relative bias (mean simulated divided by mean observed), and γ is the variability ratio (standard deviation of simulated divided by standard deviation of observed). QO_l and QS_l are the bottom 30% observed and simulated flow values. Q_{min} is the minimum flow value in the observed and simulated timeseries. μ_{obs} and μ_{sim} are the means of observed and simulated flow values.**

Metric	Description	Range (Perfect)	Equation
r_s	Spearman's rho	-1 to 1 (1)	$r_s = 1 - \frac{6 \sum d_i^2}{n \times (n^2 - 1)} \quad (1)$
rSD	Relative Standard Deviation	0 to Inf (1)	$rSD = \frac{\sigma_{sim}}{\sigma_{obs}} \quad (2)$
%Bias	Percent Bias	-100 to Inf (0)	$\%Bias = 100 \times \frac{\sum_{i=1}^N (QS_i - QO_i)}{\sum_{i=1}^N QO_i} \quad (3)$
KGE	Kling-Gupta Efficiency	-Inf to 1 (1)	$KGE = 1 - \sqrt{(r - 1)^2 + (\beta - 1)^2 + (\gamma - 1)^2} \quad (4)$
%BiasFLV	Low-flow Percent Bias	-100 to Inf (0)	$\%BiasFLV = 100 \times \left(\frac{\sum_{l=1}^L \log \left(\frac{QS_l}{Q_{min}} \right)}{\sum_{l=1}^L \log \left(\frac{QO_l}{Q_{min}} \right)} - 1 \right) \quad (5)$

%BiasFHV	High-flow Percent Bias	-100 to Inf (0)	$\%BiasFHV = 100 \times \frac{\sum_{h=1}^N (QS_h - QO_h)}{\sum_{h=1}^N QO_h} \quad (6)$
τ	Time lag	≥ 0 (0)	Corresponds to the maximum value of the cross-correlation r_τ : $r_\tau = \frac{\sum_{i=1}^{n-\tau} (QO_i - \mu_{obs}) \times (QS_{i+\tau} - \mu_{sim})}{\sqrt{\sum_{i=1}^{n-\tau} (QO_i - \mu_{obs})^2 \sum_{i=1}^{n-\tau} (QS_{i+\tau} - \mu_{sim})^2}} \quad (7)$

3 Results and discussion

Before comparing the performances of CaMa-Flood and WRF-Hydro models, driven by a regional coupled model ENEA-REG, we first present their simulated discharge time series, alongside observations and the discharge simulated by the ENEA-REG-driven HD model at both 0.5-degree and 5-minute spatial resolutions. These results are shown in Fig. 2 for a representative subset of basins, with the full set of basins provided in Fig. S4 in the Supplement. The higher-resolution HD configuration is intended to improve the representation of the drainage network and catchment area, thereby enhancing discharge estimates. However, both HD versions show a clear underestimation of freshwater inflow to the Mediterranean Sea and fail to reproduce the observed temporal patterns.

Quantitatively, the HD model exhibits very poor performance across Mediterranean basins. At 0.5-degree, the overall average KGE is -0.13 , with a mean bias of -37.4% , a Spearman's correlation of 0.36 , and a relative SD of only 0.23 . At 5-minute, the performance improves slightly (KGE = 0.00 ; %Bias = -16.6% ; $r_s = 0.48$), but variability remains strongly damped ($rSD = 0.25$). The most critical shortcoming is the systematic underestimation of extremes: high-flow biases reach -70.3% (0.5-degree) and -65.7% (5-minute), while low-flow biases are also negative (-25.3% and -9.2% , respectively). Model performances at the basin scale for both HD versions (0.5-degree and 5-minute) are provided in Tables S5 and S6 of the Supplement, respectively, offering basin-specific details beyond the aggregated statistics presented here.

These results suggest that the underestimation of freshwater inflow by the HD model is not primarily due to the long-term mean bias—which is moderate in the 5-minute configuration—but rather to its inability to capture discharge variability and high-flow peaks.

In contrast, visually WRF-Hydro and CaMa-Flood reproduce observed temporal dynamics much more closely, including variability and extremes, and therefore clearly outperform the HD model. Both models show strong potential for capturing observed patterns when using runoff from the Noah-MP land surface model—the default LSM in many Euro-Mediterranean regional coupled and Earth system models—which has already been validated against ERA5-Land runoff data (Hamitouche et al., 2025a). This indicates that CaMa-Flood and WRF-Hydro are suitable alternatives to replace the HD model in this

345 modelling framework, despite some visual biases in low- and high-flow reproduction. The following section provides a detailed evaluation of their performances.



Figure 2: Observed and simulated daily discharge for the Ebro, Rhone, Tiber, Goeksu and Po rivers for common 10 years from 1995 to 2004. Simulations include ENEA-REG-driven WRF-Hydro and CaMa-Flood, as well as the HD model at 0.5-degree and 5-minute spatial resolutions, evaluated near the corresponding gauge stations.

350 3.1 WRF-Hydro vs. CaMa-Flood (default configurations)

In this section, we compare the performance of CaMa-Flood and WRF-Hydro in its default configuration, while a detailed discussion of the calibrated WRF-Hydro is provided in the next section.

Overall, the two models, driven by a regional coupled model (i.e. ENEA-REG), show comparable skill in reproducing flow timing, but differ systematically in their ability to capture variability and discharge magnitude. CaMa-Flood tends to
355 underestimate flow variability and both high- and low-flow magnitudes, while WRF-Hydro typically produces more realistic variability, though sometimes with excessive peaks and overestimation. Both models outperform the HD baseline included in ENEA-REG, demonstrating clear added value; however, neither model performs consistently well across all Mediterranean basins, and each shows strengths and weaknesses depending on basin characteristics and scale (Figs. 3–5).

Both models reproduce the seasonal flow timing reasonably well (Fig. 3). Their mean (0.64 for CaMa-Flood vs. 0.63 for
360 WRF-Hydro) and median (0.64 for CaMa-Flood vs. 0.65 for WRF-Hydro) Spearman’s rho values are nearly identical, confirming that neither model has a systematic advantage in timing skill. Differences emerge at the basin level: WRF-Hydro excels in large basins such as the Danube, while CaMa-Flood performs better in smaller or steep catchments such as the Goeksu. The time-lag analysis (Table 2) reinforces this pattern: WRF-Hydro generally produces shorter delays in peak flow (with an average of 4.8 days vs. 8.5 days)—except in a few basins where CaMa-Flood achieves near-perfect timing. The
365 striking 43-day lag in the Danube for the CaMa-Flood aligns with findings from by Hamitouche et al. (2025a). By analysing the ENEA-REG and WRF-Hydro simulated runoffs (Fig. S5 in the supplement), we observed a close alignment in timing, indicating that the coupling of the land surface model and routing in WRF-Hydro does not significantly affect runoff timing. This suggests that the substantial lag in CaMa-Flood is primarily due to its routing limitations.

Arno	6	6
Kopru	1	4
Ebro	10	7

375 The two models diverge more substantially in representing flow variability (Fig. 3). CaMa-Flood consistently underestimates variability, often falling below the acceptable 0.8–1.2 range (Lin et al, 2019; Sanchez Lozano et al, 2025). WRF-Hydro displays a broader distribution, with several basins close to observed variability, but also instances of pronounced overestimation, especially in steep alpine basins (e.g., Adige). This contrast reflects inherent differences between a quasi-2D (solely) total runoff routing model (CaMa-Flood) and a process-based distributed system (WRF-Hydro), whose
380 representation of soil–vegetation–atmosphere processes can amplify runoff responses and lead to stronger variability signatures.

Both models show a general tendency to underestimate discharge, but CaMa-Flood does so more strongly (Fig. 3). WRF-Hydro achieves lower overall bias (-12.1% vs. -27.8%) but occasionally produces substantial overestimations in some basins—particularly where variability is already high. CaMa-Flood, by contrast, displays more uniform behaviour:
385 predominantly negative biases and limited ability to reproduce high flows. These opposite tendencies explain why WRF-Hydro performs better in some mid-size basins, while CaMa-Flood offers more stable (but typically conservative) estimates. KGE values across basins fall largely within the intermediate category ($0.30 < KGE \leq 0.65$; adapted from (Sanchez Lozano et al, 2025)) for both ENEA-REG–driven models (Fig. 4), showing that neither system consistently outperforms the other. WRF-Hydro reaches its best performance in large temperate basins, while CaMa-Flood excels in some smaller
390 Mediterranean catchments. Notably, both models improve upon the HD model included in ENEA-REG, demonstrating the benefit of dedicated routing schemes over the simpler baseline.

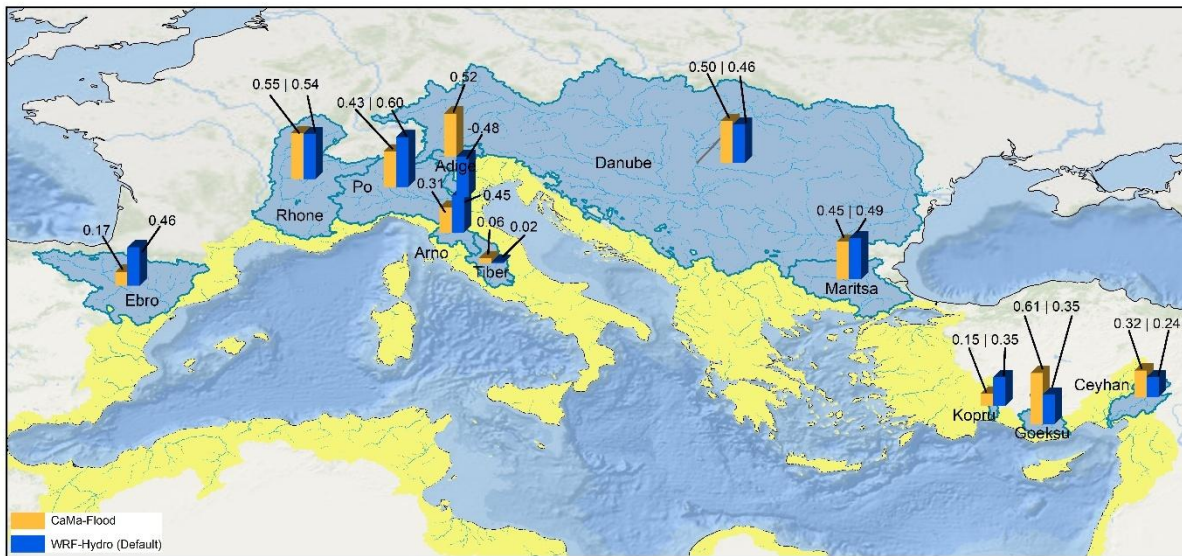


Figure 4: KGE values of each model experiment (CaMa-Flood vs. WRF-Hydro (Default)) across the studied basins.

395 Regarding low-flow and high-flow biases, these hydrological signatures evaluate performance using two segments of the flow duration curve (FDC) (Smakhtin, 2001; Vogel and Fennessey, 1994), as defined by Yilmaz et al. (2008). The high-flow segment (0–0.02 exceedance probabilities) represents watershed response to large precipitation events (Fig. S6 in the supplement) and is used to calculate high-flow bias (%BiasFHV, Eq. (6)). The low-flow segment (0.7–1.0 exceedance probabilities) reflects long-term flow sustainability (Fig. S7 in the supplement) and is used to calculate low-flow bias
400 (%BiasFLV, Eq. (5)).

High-flow and low-flow biases reveal complementary strengths (Fig. 5). CaMa-Flood systematically underestimates both extremes (-27.8% and -16.3%, respectively), reflecting a more damped hydrological response. WRF-Hydro shows more variable behaviour: it reduces high-flow underestimation on average (-2.1%) but can overestimate peak flows in certain basins, while its low-flow errors range from strong underestimation to slight overestimation, with an average of -18.0%.
405 These contrasting patterns indicate that WRF-Hydro generates a more dynamic flow regime, whereas CaMa-Flood tends toward smoother hydrographs.

helps to explain the underlying trade-offs in model performance across Mediterranean basins. CaMa-Flood tends to produce smoother hydrographs with smaller bias in some basins but underestimates variability and extremes, whereas WRF-Hydro more accurately captures flow timing and variability but occasionally overestimates peak flows.

430 These trade-offs have practical implications for different applications. For ocean–land coupling and improving mean freshwater fluxes into the Mediterranean, CaMa-Flood may be sufficient due to its stable estimates of flow volumes. For extremes prediction, which focuses on high- and low-flow events relevant to short-term forecasting and risk assessment, WRF-Hydro is generally better suited due to its richer process representation, more dynamic flow regime, and ability to capture peak flows. CaMa-Flood retains the advantage of simulating floodplain dynamics, including flood depth and extent, which is valuable for flood hazard assessment in smaller or steep catchments. For projections of future hydrological impacts
435 under climate change, which rely on climate model forcings and often assume stationarity of biases over time, both models are appropriate, as moderate differences in extremes do not strongly affect long-term water balance. Additionally, WRF-Hydro is particularly suitable for studies investigating precipitation–soil moisture feedbacks, as it allows full coupling between soil hydrology and the atmosphere, capturing critical land–atmosphere interactions.

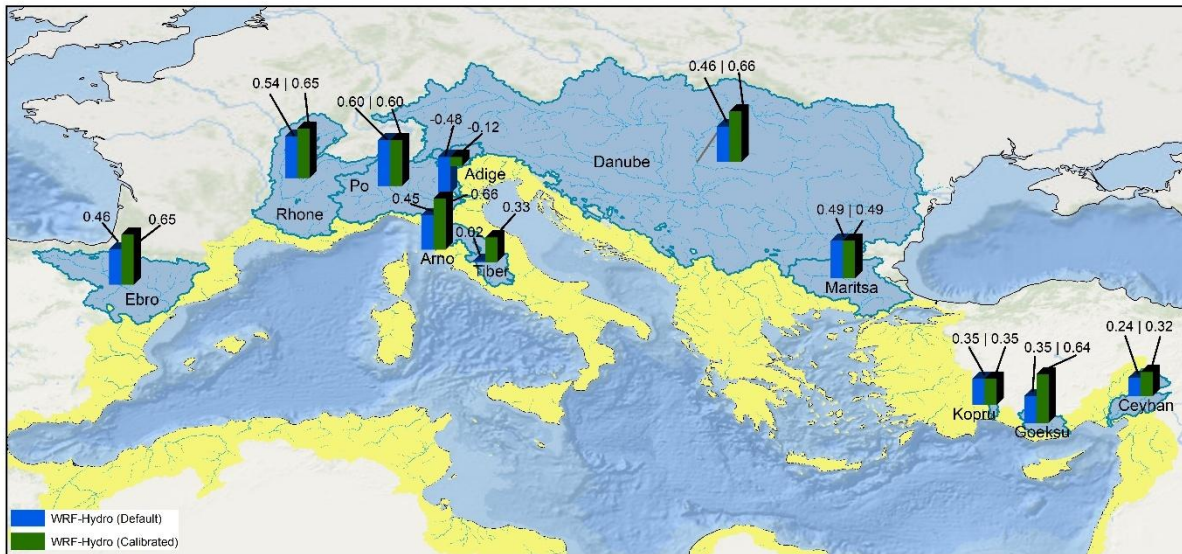
Basin characteristics further influence model suitability: WRF-Hydro performs well in large temperate basins, while CaMa-
440 Flood provides stable, conservative estimates in smaller or steep catchments. Overall, model choice should be guided by the intended application, basin characteristics, and the balance between process detail and computational efficiency.

While this study provides a systematic comparison between CaMa-Flood and WRF-Hydro, it is important to underscore that the two models are not driven by identical types of inputs. CaMa-Flood receives total runoff from Noah-MP within the ENEA-REG framework, which in our configuration is provided at daily resolution, although the model can also operate with
445 higher-frequency inputs such as hourly runoff. In contrast, WRF-Hydro uses atmospheric fields generated by ENEA-REG at 6-hourly resolution to internally compute runoff through its embedded Noah-MP land-surface model, even though it is likewise capable of operating with finer-scale atmospheric forcing. Consequently, differences in simulated discharge reflect the combined influence of both runoff generation and routing processes. For this reason, the comparison should not be interpreted as a purely hydrological benchmark in which both systems operate under identical inputs. Instead, it reflects how
450 each model performs within the coupling configuration in which it would realistically operate in a regional climate or Earth system modelling environment. In such frameworks, CaMa-Flood is typically coupled downstream of a land-surface model, while WRF-Hydro employs its own land-surface component driven directly by meteorological fields. Forcing both models with identical runoff inputs would not represent their intended operational use and would fall outside the scope of this study. Our aim was therefore to assess their relative suitability and behaviour in configurations consistent with their implementation
455 within regional coupled systems such as ENEA-REG.

3.2 WRF-Hydro calibration: performance improvements and related hydrological impacts

3.2.1 Performance metrics before and after Calibration

The calibration of WRF-Hydro, aimed to optimize the Kling-Gupta Efficiency (KGE), leads to an improvement of the model performances in most of the basins and metrics. In average, the calibration improved the KGE from 0.32 to 0.48, with the median increasing from 0.45 to 0.60. The quality of performance pass from intermediate to good (KGE > 0.6; adapted from (Sanchez Lozano et al, 2025)) in several basins such as the Arno, the Danube, the Rhone and the Ebro. After calibration, Goeksu and Tiber rivers show intermediate performance, while for the Po, Kopru, and Maritsa basins the KGE remained unchanged (Fig. 6).

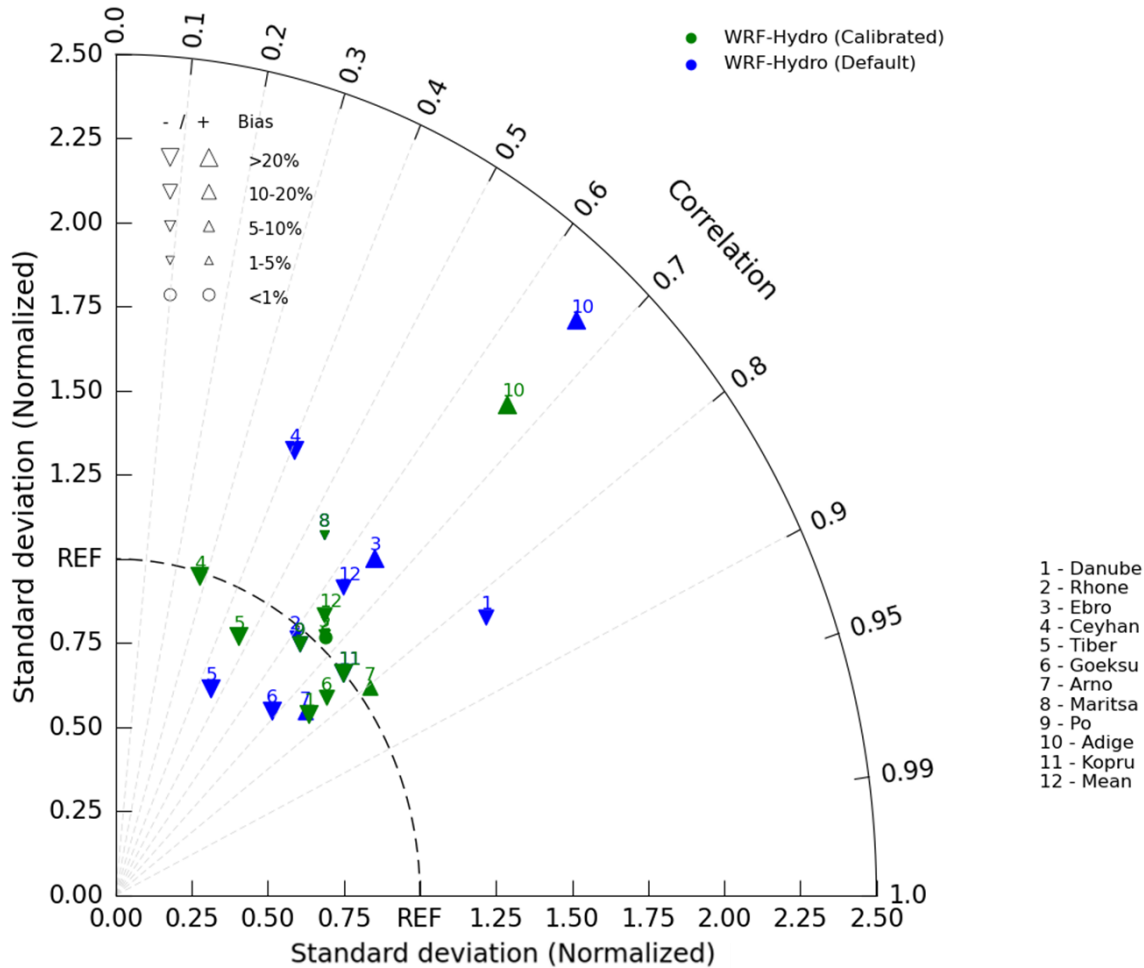


465 **Figure 6: Comparison of KGE values between the calibrated and non-calibrated WRF-Hydro model experiments across the selected basins.**

These unchanged KGE values are particularly noteworthy. They suggest that the default parameters for these basins were already close to optimal, and further calibration did not yield any improvements. This outcome highlights the robustness of the default parameter configuration in specific contexts and emphasizes the need for calibration strategies that are sensitive to basin-specific hydrological characteristics.

The components of the KGE offer further insight into these outcomes. The temporal correlation showed relative stability across most basins, with modest improvements in the Goeksu, Rhone and Arno, while noticeable declines were found in the Ceyhan. These results indicate that the improved temporal alignment between modelled and observed discharges is not systematic for all basins. In terms of bias, calibration yielded mixed results: the bias reduced substantially for the Goeksu (-33%) and the Rhone (-8.2%) basins, while worsen in the Danube (+4.6%) and the Ceyhan (+8.2%). These changes illustrate that while calibration reduced bias in many cases, it occasionally introduced trade-offs. The standard deviation also exhibited

changes with an average decreased from 1.18 to 1.08, suggesting improved consistency between simulated and observed flow variability. Relevant improvements were seen in basins such as the Danube, Ceyhan, and Arno (Fig. 7).



480 **Figure 7: Taylor diagram showing the performance of WRF-Hydro (Default, blue) and WRF-Hydro (Calibrated, green) models, driven by a regional coupled model (ENEA-REG), in different river basins numerated from 1 to 11. Number 12 refers to the mean value. The size and the orientation of the triangles represent the magnitude and under- or overestimation of the percent bias.**

In addition to these core metrics, calibration also influenced lag time (Table 3), low-flow bias, and high-flow bias (Fig. 8). Lag time improved noticeably with the average decreasing from 4.8 to 2 days. The Rhone, Ceyhan, and Arno showed substantial reductions, achieving zero lag time after calibration, while slight increases were observed in basins like the Danube. Low-flow bias exhibited minor overall improvement, shifting in average from -18.0% to -17.3%, with notable reductions in the Rhone and Goeksu basins, but with a worsening in Ceyhan. High-flow bias, on the other hand, displayed mixed results: a reduction of the extreme positive biases in the Danube and the Ceyhan together with a slight worsening in the Adige basin.

485

490 **Table 3: Summary of time lag values for the calibrated and non-calibrated WRF-Hydro model experiments in each basin.**

Basin	WRF-Hydro (Default parameters)	WRF-Hydro (Calibrated)
Danube	0	3
Rhone	6	1
Po	2	
Ceyhan	3	0
Adige	3	0
Tiber	9	0
Maritsa	7	
Goeksu	6	3
Arno	6	0
Kopru	4	
Ebro	7	0

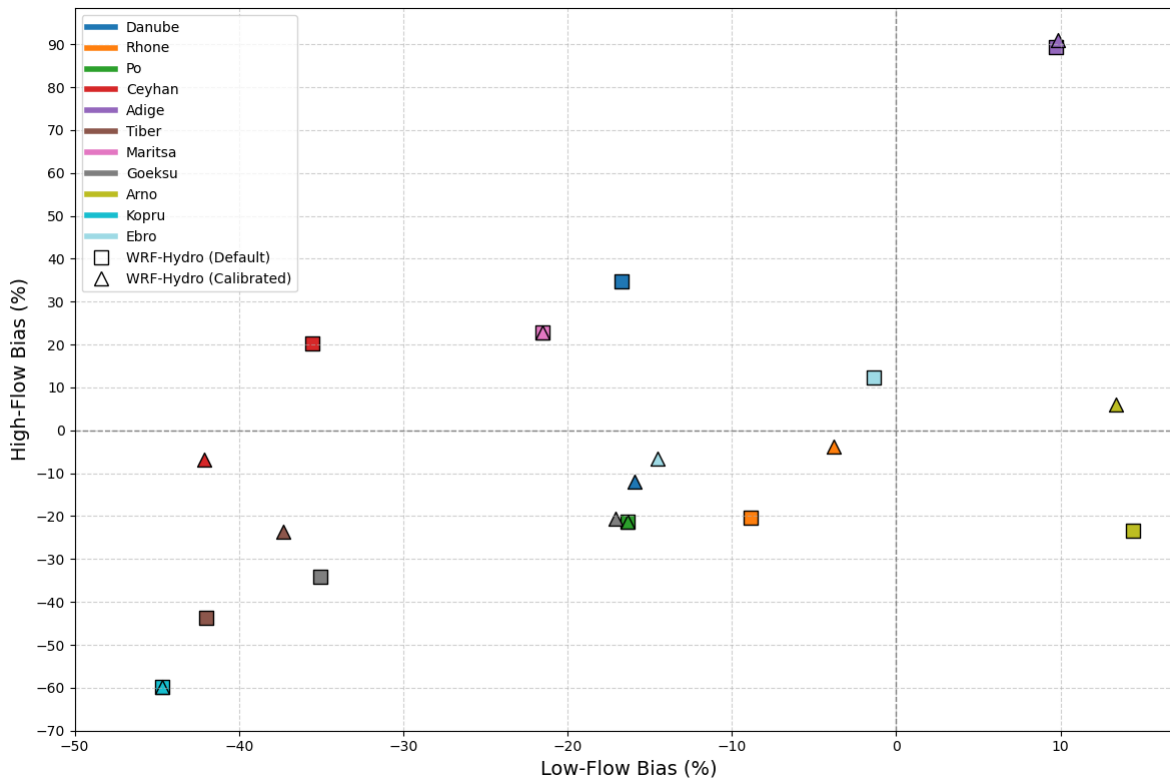


Figure 8: Scatterplot of low-flow bias vs. high-flow bias for the calibrated and non-calibrated WRF-Hydro model experiments in each river basin.

495 Overall, the calibration of WRF-Hydro enhanced discharge simulations for many Mediterranean basins, as reflected in the improvements in KGE and reductions in lag time. However, the trade-offs between correlation, bias, and standard deviation, along with the basin-specific variability, highlight areas where the calibration strategy could be refined to better capture the unique dynamics of each basin.

For the Adige basin, the poor performance, both with default and calibrated WRF-Hydro, observed particularly for the strong
 500 overestimation of high-flow events, the overall bias, and the variability, resulting in a very poor KGE, can be explained by the substantial corrections made to the drainage network. To disconnect the Adige basin from the adjacent Po River basin—necessary due to the coarse spatial resolution of the model—elevation reconditioning was applied. However, these corrections altered the topography slope, a critical factor in discharge calculations. The changes to the slope resulted in
 505 overly fast flows, which in turn caused exaggerated high-flow peaks and impacted the model's ability to simulate discharge accurately for the Adige basin. This finding underscores the sensitivity of WRF-Hydro, as any other hydrodynamic or hydrological model, to topography and the need for careful elevation reconditioning, particularly at coarse spatial resolutions. While such corrections are essential to accurately delineate basin boundaries and drainage networks, they must be implemented cautiously to avoid introducing errors that affect hydrological dynamics.

Excluding the Adige basin from the analysis demonstrated notable improvements in the overall performance of the WRF-Hydro model outperforming CaMa-Flood (Fig. 9). For instance, the calibrated WRF-Hydro configuration showed an increase in KGE from 0.48 (including Adige) to 0.53 (excluding Adige), compared to the default settings (0.32 and 0.4 respectively) and CaMa-Flood (0.37). Similarly, the percent bias improved from 23.9% to 21.5%, and the relative standard deviation became closer to 1, indicating better approximation of flow variability. These improvements underscore the sensitivity of WRF-Hydro's performance to accurate input parameters and the profound impact of specific basin corrections on overall model results.

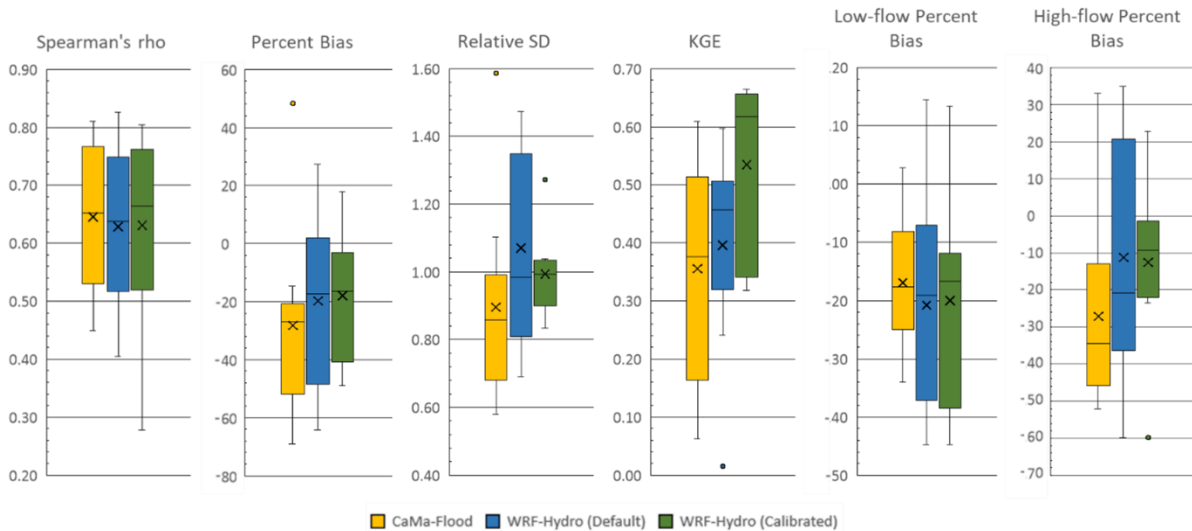


Figure 9: Performance metrics for each model experiment (with Adige basin excluded). The X represents the mean value.

It is worth noting that while some metrics, such as high-flow bias, showed a decrease in performance, this is primarily because the Adige basin's overestimation of high flows compensated for the negative biases in other basins. Nevertheless, the improvements in the key metrics—KGE, Percent Bias, and relative standard deviation—demonstrate the importance of addressing basin-specific challenges to enhance model reliability.

Post-calibration improvement was actually expected, particularly because several important sources of structural and input uncertainty are not explicitly represented in our modelling framework.

First, none of the models account for human interventions such as reservoirs, hydropower operations, and water withdrawals, which can substantially modify the timing, magnitude, and variability of streamflow in many Mediterranean rivers. This omission is primarily due to the lack of consistent and comprehensive information on reservoir characteristics and management practices across all Mediterranean basins, which span multiple countries and governance systems. Consequently, the simulated discharge reflects a naturalized flow regime, whereas the observations often reflect regulated conditions, a well-documented issue for most Mediterranean rivers (Grill et al., 2019). This inherent mismatch contributes to discrepancies in low-flow periods, peak attenuation, and seasonal timing.

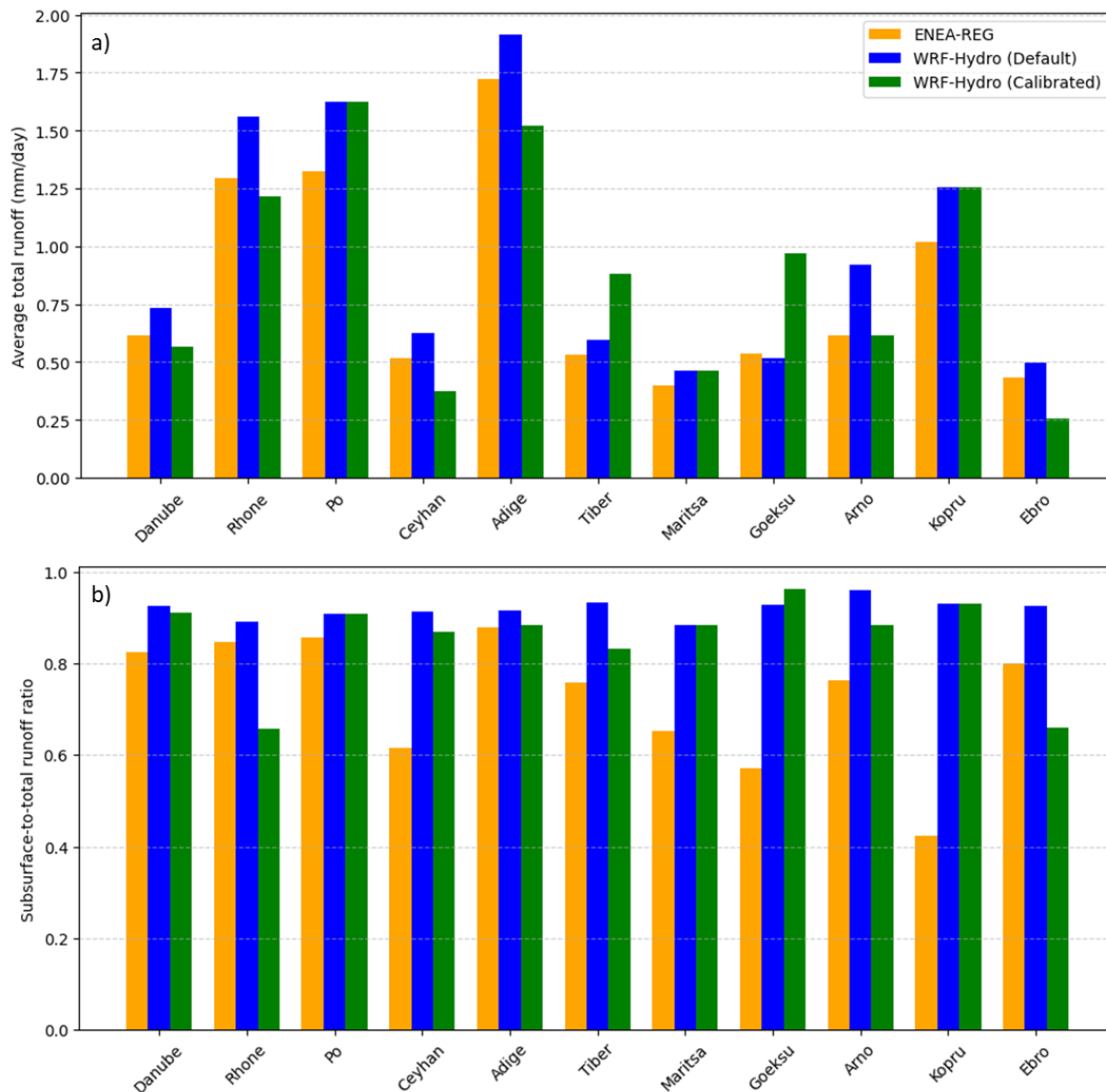
Second, locally calibrated scores help compensate for errors in catchment boundaries (Kauffeldt et al., 2013; Lehner, 2012), primarily due to the coarse resolution of elevation data, as exemplified by the Adige basin. From a purely hydrological perspective, this resolution is inadequate, and a higher resolution on the order of hundreds of meters would be preferable to better represent small basins. However, this is constrained by the very high computational resources required for simulations
535 covering a large domain, such as Med-CORDEX.

Third, calibration also mitigates errors in meteorological forcing, particularly in precipitation data (Beck et al., 2017, 2019), as shown in Sect. S1 and Fig. S8 in the supplement. The regional coupled models generate meteorological forcing at relatively coarse spatiotemporal resolution and rely on parameterized convection, known source of uncertainty and errors. In contrast, convection-permitting models, km-scale models that explicitly resolve deep convection, can more realistically
540 represent sub-daily statistics and extreme events (Fosser et al., 2024; Struglia et al., 2025), highlighting an additional limitation of regional models in capturing high-flow and short-duration extremes. Further efforts in bias correction or data assimilation of climate forcing could improve hydrological model performance, pending the extension of convection-permitting models to large domains such as Med-CORDEX, given the substantial computational resources required.

Readers should interpret the findings within this context, and future work incorporating anthropogenic controls, higher-
545 resolution runs, and refined meteorological forcing could further improve model performance.

3.2.2 Effects of calibration on runoff generation and partitioning

To better understand the source of performance improvements following calibration, we investigated how the calibrated parameters influenced key hydrological processes—particularly runoff generation and the surface–subsurface flow partitioning. This analysis helps explain the hydrological changes driving model behaviour across the Mediterranean basins.
550 Specifically, we examined simulated total runoff, as it serves as the primary input for CaMa-Flood, and the ratio of subsurface to total runoff. As a reminder, runoff is simulated by the Noah-MP land surface model, which is integrated within WRF-Hydro and embedded in WRF—used to dynamically downscale ERA5 data within the ENEA-REG coupled model. Details on the calibrated parameters, their roles in controlling hydrological processes, and trends across basins are provided in the Supplement (Sect. S2 and Table S7), while Fig. 10 summarizes and compares the average daily total runoff (mm/day)
555 and the subsurface-to-total runoff ratio simulated by the ENEA-REG model, and by WRF-Hydro using both default and calibrated parameter values. This comparison is essential for understanding the observed performance differences between the CaMa-Flood and WRF-Hydro models, alongside the distinct routing configurations in each model.



560 **Figure 10: Comparison of a) average daily total runoff and b) the ratio of subsurface to total runoff across each river basin as simulated by ENEA-REG (orange), WRF-Hydro with default parameters (blue), and WRF-Hydro with calibrated parameters (green).**

Our results indicate that WRF-Hydro (default) predominantly generate higher runoff compared to ENEA-REG, with percentage increases ranging from 11.1% to 49.8%, except for the Göksu basin, where it shows lower runoff by 3.6%. Similarly, the subsurface-to-total runoff ratio simulated by WRF-Hydro exceeds that of ENEA-REG across all basins, with percentage increases ranging from 4.1% to 119.9%. These findings underscore the sensitivity of runoff to the dynamic interactions between land surface models, routing processes, and the partitioning of surface and subsurface flows.

565

Excluding the Po, Maritsa, and Kopru basins—where default and calibrated parameters coincide—the calibration process (WRF-Hydro (calibrated)) led to a remarkable reduction in total runoff for most basins. This decrease, brought runoff values closer to, or even below, those simulated by ENEA-REG with an average reduction between 20.5% and 48.1%. However, in the Tiber and Göksu basins, the calibrated parameters produced a marked increase in total runoff. These variations can largely be attributed to changes in parameters that control transpiration and soil evaporation, as the slope parameter consistently decreased, limiting deep drainage.

For the subsurface-to-total runoff ratio, calibration effects varied. In the Göksu basin, there was a slight increase of 3.8%, while for other basins the ratio decreased, either marginally (e.g., Danube at -1.5%, Adige at -3.4%, and Ceyhan at -4.9%) or significantly (e.g., Rhone at -26.2% and Ebro at -28.7%). These changes stemmed from the combined influence of parameters governing infiltration and runoff partitioning. Together, the results highlight the critical role of parameter calibration in modulating both total runoff and its partitioning into surface and subsurface components, thereby influencing hydrological model performance.

580 **4 Conclusions**

This study assessed whether WRF-Hydro and CaMa-Flood can serve as effective alternatives to HD routing scheme for improving hydrological simulations within Euro-Mediterranean regional coupled models, and evaluated the extent to which calibration can enhance WRF-Hydro's performance.

Both models, when driven by the ENEA-REG regional coupled system, demonstrated substantial improvements over the HD baseline, particularly in reproducing temporal dynamics and discharge variability across Mediterranean basins. CaMa-Flood delivered stable, conservative estimates with consistent underestimation of variability and extremes, while WRF-Hydro exhibited a more dynamic hydrological response with generally better representation of flow timing, variability, and high-flow behaviour. However, neither model performed uniformly across all basins, reflecting the diverse hydrological regimes of the Mediterranean region. Importantly, this model comparison should be interpreted within the context of their integration into a regional coupled modelling system, rather than as a pure hydrological benchmark with identical runoff inputs or meteorological forcings.

Calibration significantly improved the performance of WRF-Hydro across most basins, increasing KGE, reducing timing lags, and improving the representation of discharge variability. These improvements were basin-dependent and were influenced by different sources of structural and input uncertainty—including the exclusion of human interventions, catchment boundary inaccuracies linked to coarse-resolution topography, and biases in precipitation forcing typical of regional climate models. The Adige basin highlighted the sensitivity of hydrodynamic models to drainage network corrections, underscoring the need for careful topographic preparation in coarse-resolution regional applications.

Overall, the findings demonstrate that both WRF-Hydro and CaMa-Flood are viable alternatives to the HD model for use in regional coupled modelling frameworks such as Med-CORDEX. WRF-Hydro provides stronger performance especially for

600 applications requiring detailed representation of variability, extremes, and land–atmosphere interactions. CaMa-Flood, with its computational efficiency and capacity to simulate floodplain dynamics, offers a robust and scalable alternative, particularly for Mediterranean basins where stable discharge estimates are sufficient.

The study also provides a calibrated parameter set for WRF-Hydro that may be transferable to hydrologically similar basins or serve as a baseline for higher-resolution applications. Future work should incorporate reservoir operations, enhanced
605 topographic representation, and improved meteorological forcing, to further advance hydrological realism in regional coupled systems.

Code and data availability

ERA5 data, provided by the European Centre for Medium-Range Weather Forecast (ECMWF), can be freely downloaded from the Copernicus Data Store (<https://doi.org/10.24381/cds.adbb2d47> (Hersbach et al., 2020)). All the model codes used in
610 our study, including ENEA-REG, WRF-Hydro, CaMa-Flood, and the WRF-Hydro calibration package, as well as the discharge observation data used for model evaluation, are available at the following permanent repository: <https://doi.org/10.5281/zenodo.16625613> (Hamitouche et al., 2025b). Model output data are available from the corresponding author upon request due to their large volume. However, a step-by-step instruction file, along with all associated materials required to reproduce the results of this study, is publicly available on Zenodo at
615 <https://doi.org/10.5281/zenodo.16333943> (Hamitouche et al., 2025c).

Author contribution

MH, GF, and AA: conceptualisation and methodology; MH: formal analysis, funding acquisition, investigation, visualisation and writing-original draft preparation; MH and AA: simulations; AR: helped with calibration setup; GF and AA: supervision; MH, GF, AA, and AR: validation and writing-review & editing. All authors have read and agreed to the
620 published version of the paper.

Competing interests

The authors declare that they have no conflict of interest.

Acknowledgements

We would like to thank Stefan Hagemann for providing us with some discharge observation data and Day Yamazaki and
625 Kevin Sampson for their valuable help in setting up the CaMa-Flood and WRF-Hydro models.

The analysis was partially carried out on the High Performance Computing DataCenter at IUSS, co-funded by Regione Lombardia through the funding programme established by Regional Decree No. 3776 of November 3, 2020.

Financial support

630 This paper and related research have been conducted during and with the support of the Italian PhD course in Sustainable Development and Climate change (link: www.phd-sdc.it) at the University School for Advanced Studies IUSS and developed within the framework of the project “Dipartimento di Eccellenza 2023-2027”, with the financial support from the ICSC Italian Research Center on High-Performance Computing, Big Data and Quantum Computing and received funding from the European Union Next-GenerationEU (National Recovery and Resilience Plan-NRRP, Mission 4, Component 2, Investment 1.4-D.D: 3138 16/12/2021, CN00000013).

635 This research has also been supported by the CIHEAM Prize for the Best MSc Thesis 2022.

References

Amelia, J.: Development of Two-Way Coupled Atmospheric Hydrological models, *Journal of Climatology & Weather Forecasting*, 11, 001-002, 2022.

640 Anav, A., Carillo, A., Palma, M., Struglia, M. V, Turuncoglu, U. U., and Sannino, G.: The ENEA-REG system (v1.0), a multi-component regional Earth system model: sensitivity to different atmospheric components over the Med-CORDEX (Coordinated Regional Climate Downscaling Experiment) region, *Geosci Model Dev*, 14, 4159–4185, <https://doi.org/10.5194/gmd-14-4159-2021>, 2021.

645 Bates, P. D., Horritt, M. S., and Fewtrell, T. J.: A simple inertial formulation of the shallow water equations for efficient two-dimensional flood inundation modelling, *J Hydrol (Amst)*, 387, 33–45, <https://doi.org/10.1016/j.jhydrol.2010.03.027>, 2010.

650 Beck, H. E., Vergopolan, N., Pan, M., Levizzani, V., van Dijk, A. I. J. M., Weedon, G. P., Brocca, L., Pappenberger, F., Huffman, G. J., and Wood, E. F.: Global-scale evaluation of 22 precipitation datasets using gauge observations and hydrological modeling, *Hydrol Earth Syst Sci*, 21, 6201–6217, <https://doi.org/10.5194/hess-21-6201-2017>, 2017.

655 Beck, H. E., Pan, M., Roy, T., Weedon, G. P., Pappenberger, F., van Dijk, A. I. J. M., Huffman, G. J., Adler, R. F., and Wood, E. F.: Daily evaluation of 26 precipitation datasets using Stage-IV gauge-radar data for the CONUS, *Hydrol Earth Syst Sci*, 23, 207–224, <https://doi.org/10.5194/hess-23-207-2019>, 2019.

Beck, H. E., Pan, M., Lin, P., Seibert, J., van Dijk, A. I. J. M., and Wood, E. F.: Global Fully Distributed Parameter Regionalization Based on Observed Streamflow From 4,229 Headwater Catchments, *Journal of Geophysical Research: Atmospheres*, 125, e2019JD031485, <https://doi.org/10.1029/2019JD031485>, 2020.

660

Casper, M. C., Grigoryan, G., Gronz, O., Gutjahr, O., Heinemann, G., Ley, R., and Rock, A.: Analysis of projected hydrological behavior of catchments based on signature indices, *Hydrol Earth Syst Sci*, 16, 409–421, <https://doi.org/10.5194/hess-16-409-2012>, 2012.

665 CEH-CEDEX: Centro de Estudios Hidrográficos del Centro de estudios y experimentación de obras públicas, Spain, <https://ceh.cedex.es> (last access: 28 April 2024), 2024.

Cerbelaud, A., Lefèvre, J., Genthon, P., and Menkes, C.: Assessment of the WRF-Hydro uncoupled hydro-meteorological model on flashy watersheds of the Grande Terre tropical island of New Caledonia (South-West Pacific), *J Hydrol Reg Stud*, 670 40, 101003, <https://doi.org/10.1016/j.ejrh.2022.101003>, 2022.

Cisterna-García, A., González-Vidal, A., Martínez-Ibarra, A., Ye, Y., Guillén-Teruel, A., Bernal-Escobedo, L., and Skarmeta, A. F.: Artificial intelligence for streamflow prediction in river basins: a use case in Mar Menor, *Sci Rep*, 15, 19481, <https://doi.org/10.1038/s41598-025-04524-0>, 2025.

675

Cosgrove, B., Gochis, D., Flowers, T., Dugger, A., Ogden, F., Graziano, T., Clark, E., Cabell, R., Casiday, N., Cui, Z., Eicher, K., Fall, G., Feng, X., Fitzgerald, K., Frazier, N., George, C., Gibbs, R., Hernandez, L., Johnson, D., Jones, R., Karsten, L., Kefelegn, H., Kitzmiller, D., Lee, H., Liu, Y., Mashriqui, H., Mattern, D., McCluskey, A., McCreight, J. L., McDaniel, R., Midekisa, A., Newman, A., Pan, L., Pham, C., RafieeiNasab, A., Rasmussen, R., Read, L., Rezaeianzadeh, 680 M., Salas, F., Sang, D., Sampson, K., Schneider, T., Shi, Q., Sood, G., Wood, A., Wu, W., Yates, D., Yu, W., and Zhang, Y.: NOAA’s National Water Model: Advancing operational hydrology through continental-scale modeling, *JAWRA Journal of the American Water Resources Association*, 60, 247–272, <https://doi.org/10.1111/1752-1688.13184>, 2024.

Djurdjevic, V., and Rajkovic, B.: Development of the EBU-POM coupled regional climate model and results from climate 685 change experiments, Nova, New York, 2010.

Drobinski, P., Anav, A., Lebeaupin Brossier, C., Samson, G., Stéfanon, M., Bastin, S., Baklouti, M., Béranger, K., Beuvier, J., Bourdallé-Badie, R., Coquart, L., D’Andrea, F., de Noblet-Ducoudré, N., Diaz, F., Dutay, J.-C., Ethe, C., Foujols, M.-A., Khvorostyanov, D., Madec, G., Mancip, M., Masson, S., Menut, L., Palmieri, J., Polcher, J., Turquety, S., Valcke, S., and

- 690 Viovy, N.: Model of the Regional Coupled Earth system (MORCE): Application to process and climate studies in vulnerable regions, *Environmental Modelling & Software*, 35, 1–18, <https://doi.org/10.1016/j.envsoft.2012.01.017>, 2012.
- Fosser, G., Gaetani, M., Kendon, E. J., Adinolfi, M., Ban, N., Belušić, D., Caillaud, C., Careto, J. A. M., Coppola, E., Demory, M.-E., de Vries, H., Dobler, A., Feldmann, H., Goergen, K., Lenderink, G., Pichelli, E., Schär, C., Soares, P. M. M., Somot, S., and Tölle, M. H.: Convection-permitting climate models offer more certain extreme rainfall projections, *NPJ Clim Atmos Sci*, 7, 51, <https://doi.org/10.1038/s41612-024-00600-w>, 2024.
- 695 Galanaki, E., Lagouvardos, K., Kotroni, V., Giannaros, T., and Giannaros, C.: Implementation of WRF-Hydro at two drainage basins in the region of Attica, Greece, for operational flood forecasting, *Natural Hazards and Earth System Sciences*, 21, 1983–2000, <https://doi.org/10.5194/nhess-21-1983-2021>, 2021.
- 700 Gochis, D. J., Barlage, M., Cabell, R., Casali, M., Dugger, A., Fitzgerald, K., McCallister, M., McCreight, J., RafieeiNasab, A., Read, L., Sampson, K., Yates, D., and Zhang, Y.: The WRF-Hydro Modeling System Technical Description. (Version 5.2), NCAR Technical Note, 108 pp, [https://ral.ucar.edu/sites/default/files/docs/water/wrf-hydro-v511-technical-](https://ral.ucar.edu/sites/default/files/docs/water/wrf-hydro-v511-technical-description.pdf)
705 [description.pdf](https://ral.ucar.edu/sites/default/files/docs/water/wrf-hydro-v511-technical-description.pdf) (last access: 27 February 2025), 2021.
- GRDC: Data Portal, https://grdc.bafg.de/data/data_portal/ (last access: 28 April 2024), 2024.
- Grill, G., Lehner, B., Thieme, M., Geenen, B., Tickner, D., Antonelli, F., Babu, S., Borrelli, P., Cheng, L., Crochetiere, H., Ehalt Macedo, H., Filgueiras, R., Goichot, M., Higgins, J., Hogan, Z., Lip, B., McClain, M. E., Meng, J., Mulligan, M., Nilsson, C., Olden, J. D., Opperman, J. J., Petry, P., Reidy Liermann, C., Sáenz, L., Salinas-Rodríguez, S., Schelle, P., Schmitt, R. J. P., Snider, J., Tan, F., Tockner, K., Valdujo, P. H., van Soesbergen, A., and Zarfl, C.: Mapping the world’s free-flowing rivers, *Nature*, 569, 215–221, <https://doi.org/10.1038/s41586-019-1111-9>, 2019.
- 715 Gupta, H. V., Kling, H., Yilmaz, K. K., and Martinez, G. F.: Decomposition of the mean squared error and NSE performance criteria: Implications for improving hydrological modelling, *J Hydrol (Amst)*, 377, 80–91, <https://doi.org/10.1016/j.jhydrol.2009.08.003>, 2009.
- Hagemann, S. and Dümenil, L.: A parametrization of the lateral waterflow for the global scale, *Clim Dyn*, 14, 17–31, <https://doi.org/10.1007/s003820050205>, 1997.
- 720 Hagemann, S., Stacke, T., and Ho-Hagemann, H. T. M.: High Resolution Discharge Simulations Over Europe and the Baltic Sea Catchment, *Front Earth Sci (Lausanne)*, Volume 8-2020, <https://doi.org/10.3389/feart.2020.00012>, 2020.

- 725 Hamitouche, M., Fossier, G., Anav, A., He, C., and Lin, T.-S.: Impact of runoff schemes on global flow discharge: a comprehensive analysis using the Noah-MP and CaMa-Flood models, *Hydrol Earth Syst Sci*, 29, 1221–1240, <https://doi.org/10.5194/hess-29-1221-2025>, 2025a.
- Hamitouche, M., Fossier, G., RafieeiNasab, A., Anav, A.: Model codes and observation data for "Regional-scale Hydrologic Model Comparison Including Calibration for Improved River Discharge Simulations into the Mediterranean Sea", Zenodo [model], <https://doi.org/10.5281/zenodo.16333943>, 2025b.
- 730 Hamitouche, M., Fossier, G., RafieeiNasab, A., Anav, A.: Step-by-step instructions to reproduce the results of "Regional-scale Hydrologic Model Comparison Including Calibration for Improved River Discharge Simulations into the Mediterranean Sea", Zenodo [workflow], <https://doi.org/10.5281/zenodo.16333943>, 2025c.
- Hersbach, H., Bell, B., Berrisford, P., Hirahara, S., Horányi, A., Muñoz-Sabater, J., Nicolas, J., Peubey, C., Radu, R., Schepers, D., Simmons, A., Soci, C., Abdalla, S., Abellan, X., Balsamo, G., Bechtold, P., Biavati, G., Bidlot, J., Bonavita, M., De Chiara, G., Dahlgren, P., Dee, D., Diamantakis, M., Dragani, R., Flemming, J., Forbes, R., Fuentes, M., Geer, A., Haimberger, L., Healy, S., Hogan, R. J., Hólm, E., Janisková, M., Keeley, S., Laloyaux, P., Lopez, P., Lupu, C., Radnoti, G., de Rosnay, P., Rozum, I., Vamborg, F., Villaume, S., and Thépaut, J.-N.: The ERA5 global reanalysis, *Quarterly Journal of the Royal Meteorological Society*, 146, 1999–2049, <https://doi.org/10.1002/qj.3803>, 2020.
- 740 Kauffeldt, A., Halldin, S., Rodhe, A., Xu, C.-Y., and Westerberg, I. K.: Disinformative data in large-scale hydrological modelling, *Hydrol Earth Syst Sci*, 17, 2845–2857, <https://doi.org/10.5194/hess-17-2845-2013>, 2013.
- Kiliçarslan, B. M.: Calibration and Evaluation of WRF-Hydro Modeling System for Extreme Runoff Simulations: Use of High-Resolution Sea Surface Temperature (SST) Data, Middle East Technical University (Turkey), 2022.
- 750 Knoben, W. J. M., Freer, J. E., and Woods, R. A.: Technical note: Inherent benchmark or not? Comparing Nash–Sutcliffe and Kling–Gupta efficiency scores, *Hydrol Earth Syst Sci*, 23, 4323–4331, <https://doi.org/10.5194/hess-23-4323-2019>, 2019.
- Lahmers, T. M., Gupta, H., Castro, C. L., Gochis, D. J., Yates, D., Dugger, A., Goodrich, D., and Hazenberg, P.: Enhancing the Structure of the WRF-Hydro Hydrologic Model for Semiarid Environments, *J Hydrometeorol*, 20, 691–714, <https://doi.org/10.1175/JHM-D-18-0064.1>, 2019.
- 755

Lehner, B.: Derivation of Watershed Boundaries for GRDC Gauging Stations Based on the HydroSHEDS Drainage Network; Technical Report Prepared for the GRDC, Bundesanstalt für Gewässerkunde, 2012.

760 Lin, P., Pan, M., Beck, H. E., Yang, Y., Yamazaki, D., Frasson, R., David, C. H., Durand, M., Pavelsky, T. M., Allen, G. H., Gleason, C. J., and Wood, E. F.: Global Reconstruction of Naturalized River Flows at 2.94 Million Reaches, *Water Resour Res*, 55, 6499–6516, <https://doi.org/10.1029/2019WR025287>, 2019.

Lionello, P., Abrantes, F., Congedi, L., Dulac, F., Gacic, M., Gomis, D., Goodess, C., Hoff, H., Kutiel, H., Luterbacher, J.,
765 Planton, S., Reale, M., Schröder, K., Vittoria Struglia, M., Toreti, A., Tsimplis, M., Ulbrich, U., and Xoplaki, E.: Introduction: Mediterranean Climate—Background Information, in: *The Climate of the Mediterranean Region*, edited by: Lionello, P., Elsevier, Oxford, xxxv–xc, <https://doi.org/10.1016/B978-0-12-416042-2.00012-4>, 2012.

Ludwig, W., Dumont, E., Meybeck, M., and Heussner, S.: River discharges of water and nutrients to the Mediterranean and
770 Black Sea: Major drivers for ecosystem changes during past and future decades?, *Prog Oceanogr*, 80, 199–217, <https://doi.org/10.1016/j.pocean.2009.02.001>, 2009.

Momblanch, A., Andreu, J., Paredes-Arquiola, J., Solera, A., and Pedro-Monzonís, M.: Adapting water accounting for
integrated water resource management. The Júcar Water Resource System (Spain), *J Hydrol (Amst)*, 519, 3369–3385,
775 <https://doi.org/https://doi.org/10.1016/j.jhydrol.2014.10.002>, 2014.

Pinardi, N. and Masetti, E.: Variability of the large scale general circulation of the Mediterranean Sea from observations and
modelling: a review, *Palaeogeogr Palaeoclimatol Palaeoecol*, 158, 153–173, [https://doi.org/10.1016/S0031-0182\(00\)00048-](https://doi.org/10.1016/S0031-0182(00)00048-1)
1, 2000.

780 Pinardi, N., Zavatarelli, M., Adani, M., Coppini, G., Fratianni, C., Oddo, P., Simoncelli, S., Tonani, M., Lyubartsev, V., Dobricic, S., and Bonaduce, A.: Mediterranean Sea large-scale low-frequency ocean variability and water mass formation rates from 1987 to 2007: A retrospective analysis, *Prog Oceanogr*, 132, 318–332, <https://doi.org/10.1016/j.pocean.2013.11.003>, 2015.

785 RafieeiNasab, A., Mazrooei, A., Enzminger, T., Srivastava, I., Dugger, A., Gochis, D., Omani, N., Grim, J., Sampson, K., Zhang, Y., LaFontaine, J., Viger, R., Liu, Y., and Schneider, T.: A WRF-Hydro-based retrospective simulation of water resources for US integrated water availability assessment, *Hydrology and Earth System Sciences Discussions*, 2024, 1–37, <https://doi.org/10.5194/hess-2024-262>, 2024.

790

- RafieeiNasab, A., Fienen, M. N., Omani, N., Srivastava, I., and Dugger, A. L.: Ensemble Methods for Parameter Estimation of WRF-Hydro, *Water Resour Res*, 61, e2024WR038048, <https://doi.org/10.1029/2024WR038048>, 2025.
- 795 Reale, M., Giorgi, F., Solidoro, C., Di Biagio, V., Di Sante, F., Mariotti, L., Farneti, R., and Sannino, G.: The Regional Earth System Model RegCM-ES: Evaluation of the Mediterranean Climate and Marine Biogeochemistry, *J Adv Model Earth Syst*, 12, e2019MS001812, <https://doi.org/10.1029/2019MS001812>, 2020.
- 800 Ruti, P. M., Somot, S., Giorgi, F., Dubois, C., Flaounas, E., Obermann, A., Dell'Aquila, A., Pisacane, G., Harzallah, A., Lombardi, E., Ahrens, B., Akhtar, N., Alias, A., Arsouze, T., Aznar, R., Bastin, S., Bartholy, J., Béranger, K., Beuvier, J., Bouffies-Cloch e, S., Brauch, J., Cabos, W., Calmanti, S., Calvet, J.-C., Carillo, A., Conte, D., Coppola, E., Djurdjevic, V., Drobinski, P., Elizalde-Arellano, A., Gaertner, M., Gal an, P., Gallardo, C., Gualdi, S., Goncalves, M., Jorba, O., Jord a, G., L'Heveder, B., Lebeaupin-Brossier, C., Li, L., Liguori, G., Lionello, P., Maci as, D., Nabat, P.,  onol, B., Raikovic, B., Ramage, K., Sevault, F., Sannino, G., Struglia, M. V., Sanna, A., Torma, C., and Vervatis, V.: Med-CORDEX Initiative for Mediterranean Climate Studies, *Bull Am Meteorol Soc*, 97, 1187–1208, <https://doi.org/10.1175/BAMS-D-14-00176.1>, 2016.
- 805 Sanchez Lozano, J. L., Rojas Lesmes, D. J., Romero Bustamante, E. G., Hales, R. C., Nelson, E. J., Williams, G. P., Ames, D. P., Jones, N. L., Gutierrez, A. L., and Cardona Almeida, C.: Historical simulation performance evaluation and monthly flow duration curve quantile-mapping (MFDC-QM) of the GEOGLOWS ECMWF streamflow hydrologic model, *Environmental Modelling & Software*, 183, 106235, <https://doi.org/10.1016/j.envsoft.2024.106235>, 2025.
- 810 Senatore, A., Mendicino, G., Gochis, D. J., Yu, W., Yates, D. N., and Kunstmann, H.: Fully coupled atmosphere-hydrology simulations for the central Mediterranean: Impact of enhanced hydrological parameterization for short and long time scales, *J Adv Model Earth Syst*, 7, 1693–1715, <https://doi.org/10.1002/2015MS000510>, 2015.
- 815 Shahi, N. K., Polcher, J., Bastin, S., Pennel, R., and Fita, L.: Assessment of the spatio-temporal variability of the added value on precipitation of convection-permitting simulation over the Iberian Peninsula using the RegIPSL regional earth system model, *Clim Dyn*, 59, 471–498, <https://doi.org/10.1007/s00382-022-06138-y>, 2022.
- 820 Smakhtin, V. U.: Low flow hydrology: a review, *J Hydrol (Amst)*, 240, 147–186, [https://doi.org/10.1016/S0022-1694\(00\)00340-1](https://doi.org/10.1016/S0022-1694(00)00340-1), 2001.
- Sofokleous, I., Bruggeman, A., Camera, C., and Eliades, M.: Grid-based calibration of the WRF-Hydro with Noah-MP model with improved groundwater and transpiration process equations, *J Hydrol (Amst)*, 617, 128991, <https://doi.org/10.1016/j.jhydrol.2022.128991>, 2023.

825

Sofokleous, I., Bruggeman, A., and Camera, C.: The Role of Parameterizations and Model Coupling on Simulations of Energy and Water Balances – Investigations With the Atmospheric Model WRF and the Hydrologic Model WRF-Hydro, *Journal of Geophysical Research: Atmospheres*, 129, e2023JD040335, <https://doi.org/10.1029/2023JD040335>, 2024.

830 Spearman, C.: The Proof and Measurement of Association between Two Things, *Am J Psychol*, 15, 72–101, <https://doi.org/10.2307/1412159>, 1904.

Stacke, T. and Hagemann, S.: HydroPy (v1.0): a new global hydrology model written in Python, *Geosci Model Dev*, 14, 7795–7816, <https://doi.org/10.5194/gmd-14-7795-2021>, 2021.

835

Storto, A., Hesham Essa, Y., de Toma, V., Anav, A., Sannino, G., Santoleri, R., and Yang, C.: MESMAR v1: a new regional coupled climate model for downscaling, predictability, and data assimilation studies in the Mediterranean region, *Geosci Model Dev*, 16, 4811–4833, <https://doi.org/10.5194/gmd-16-4811-2023>, 2023.

840 Struglia, M. V., Mariotti, A., and Filograsso, A.: River Discharge into the Mediterranean Sea: Climatology and Aspects of the Observed Variability, *J Clim*, 17, 4740–4751, <https://doi.org/10.1175/JCLI-3225.1>, 2004.

Struglia, M. V, Anav, A., Antonelli, M., Calmanti, S., Catalano, F., Dell’Aquila, A., Pichelli, E., and Pisacane, G.: Impact of spatial resolution on multi-scenario WRF-ARW simulations driven by the CMIP6 MPI-ESM1-2-HR global model: a focus on precipitation distribution over Italy, *Geosci Model Dev*, 18, 6095–6116, <https://doi.org/10.5194/gmd-18-6095-2025>, 2025.

Suárez-Almiñana, S., Pedro-Monzonís, M., Paredes-Arquiola, J., Andreu, J., and Solera, A.: Linking Pan-European data to the local scale for decision making for global change and water scarcity within water resources planning and management, *Science of The Total Environment*, 603–604, 126–139, <https://doi.org/https://doi.org/10.1016/j.scitotenv.2017.05.259>, 2017.

850

Tijerina-Kreuzer, D., Condon, L., FitzGerald, K., Dugger, A., O’Neill, M. M., Sampson, K., Gochis, D., and Maxwell, R.: Continental Hydrologic Intercomparison Project, Phase 1: A Large-Scale Hydrologic Model Comparison Over the Continental United States, *Water Resour Res*, 57, e2020WR028931, <https://doi.org/10.1029/2020WR028931>, 2021.

855

Tolson, B. A. and Shoemaker, C. A.: Dynamically dimensioned search algorithm for computationally efficient watershed model calibration, *Water Resour Res*, 43, <https://doi.org/10.1029/2005WR004723>, 2007.

- 860 Verma, K. and J., I.: Applicability of SWOT data in calibrating WRF-Hydro hydrological model over the Tawa River basin, *Geocarto Int*, 38, 2185292, <https://doi.org/10.1080/10106049.2023.2185292>, 2023.
- 865 Verri, G., Pinardi, N., Gochis, D., Tribbia, J., Navarra, A., Coppini, G., and Vukicevic, T.: A meteo-hydrological modelling system for the reconstruction of river runoff: the case of the Ofanto river catchment, *Nat. Hazards Earth Syst. Sci.*, 17, 1741–1761, <https://doi.org/10.5194/nhess-17-1741-2017>, 2017.
- Vogel, R. M. and Fennessey, N. M.: Flow-Duration Curves. I: New Interpretation and Confidence Intervals, *J Water Resour Plan Manag*, 120, 485–504, [https://doi.org/10.1061/\(ASCE\)0733-9496\(1994\)120:4\(485\)](https://doi.org/10.1061/(ASCE)0733-9496(1994)120:4(485)), 1994.
- 870 Wu, H., Kimball, J. S., Li, H., Huang, M., Leung, L. R., and Adler, R. F.: A new global river network database for macroscale hydrologic modeling, *Water Resour Res*, 48, <https://doi.org/10.1029/2012WR012313>, 2012.
- 875 Yamazaki, D., Oki, T., and Kanae, S.: Deriving a global river network map and its sub-grid topographic characteristics from a fine-resolution flow direction map, *Hydrol Earth Syst Sci*, 13, 2241–2251, <https://doi.org/10.5194/hess-13-2241-2009>, 2009.
- Yamazaki, D., Kanae, S., Kim, H., and Oki, T.: A physically based description of floodplain inundation dynamics in a global river routing model, *Water Resour Res*, 47, <https://doi.org/10.1029/2010WR009726>, 2011.
- 880 Yamazaki, D., Baugh, C. A., Bates, P. D., Kanae, S., Alsdorf, D. E., and Oki, T.: Adjustment of a spaceborne DEM for use in floodplain hydrodynamic modeling, *J Hydrol (Amst)*, 436–437, 81–91, <https://doi.org/10.1016/j.jhydrol.2012.02.045>, 2012.
- 885 Yamazaki, D., de Almeida, G. A. M., and Bates, P. D.: Improving computational efficiency in global river models by implementing the local inertial flow equation and a vector-based river network map, *Water Resour Res*, 49, 7221–7235, <https://doi.org/10.1002/wrcr.20552>, 2013.
- 890 Yamazaki, D., Ikeshima, D., Sosa, J., Bates, P. D., Allen, G. H., and Pavelsky, T. M.: MERIT Hydro: A High-Resolution Global Hydrography Map Based on Latest Topography Dataset, *Water Resour Res*, 55, 5053–5073, <https://doi.org/10.1029/2019WR024873>, 2019.
- Yilmaz, K. K., Gupta, H. V., and Wagener, T.: A process-based diagnostic approach to model evaluation: Application to the NWS distributed hydrologic model, *Water Resour Res*, 44, <https://doi.org/10.1029/2007WR006716>, 2008.

895 Yu, E., Liu, X., Li, J., and Tao, H.: Calibration and Evaluation of the WRF-Hydro Model in Simulating the Streamflow over
the Arid Regions of Northwest China: A Case Study in Kaidu River Basin, *Sustainability*, 15,
<https://doi.org/10.3390/su15076175>, 2023.

900 Yue, S., Pilon, P., and Cavadias, G.: Power of the Mann–Kendall and Spearman’s rho tests for detecting monotonic trends in
hydrological series, *J Hydrol (Amst)*, 259, 254–271, [https://doi.org/10.1016/S0022-1694\(01\)00594-7](https://doi.org/10.1016/S0022-1694(01)00594-7), 2002.

Zavatarelli, M., Raicich, F., Bregant, D., Russo, A., and Artegiani, A.: Climatological biogeochemical characteristics of the
Adriatic Sea, *Journal of Marine Systems*, 18, 227–263, [https://doi.org/10.1016/S0924-7963\(98\)00014-1](https://doi.org/10.1016/S0924-7963(98)00014-1), 1998.